Ring comb copolymer brushes

ARTICLE *in* THE JOURNAL OF CHEMICAL PHYSICS · NOVEMBER 2000

Impact Factor: 2.95 · DOI: 10.1063/1.1311964 · Source: OAI

3 AUTHORS, INCLUDING:

Andrey V Subbotin
Russian Academy of Sciences
57 PUBLICATIONS **888** CITATIONS
SEE PROFILE

G. ten Brinke
University of Groningen
280 PUBLICATIONS **9,409** CITATIONS
SEE PROFILE

Ring comb copolymer brushes

Edwin Flikkema
Department of Polymer Science and Materials Science Centre, University of Groningen, Nijenborgh 4, 9747 AG Groningen, The Netherlands

Andrei Subbotin
Department of Polymer Science and Materials Science Centre, University of Groningen, Nijenborgh 4, 9747 AG Groningen, The Netherlands and Institute of Petrochemical Synthesis, Russian Academy of Sciences, Moscow 117912, Russia

Gerrit ten Brinke
Department of Polymer Science and Materials Science Centre, University of Groningen, Nijenborgh 4, 9747 AG Groningen, The Netherlands

(Received 7 June 2000; accepted 1 August 2000)

The equilibrium conformations of isolated comb copolymer ring molecules in an athermal solution are investigated by off-lattice Monte Carlo simulations. The molecules considered consist of a closed flexible backbone densely grafted with flexible or rigid side chains. The study focuses on the influence of the length of the side chains on the conformational behavior. As a function of the side chain length the structure gradually stiffens until the size of the side chains approaches the diameter of the ring. Longer side chains do not influence the backbone conformation any further. The results are compared with the large body of knowledge available for linear cylindrical comb copolymer brushes. © *2000 American Institute of Physics.* [S0021-9606(00)50141-X]

I. INTRODUCTION

Shape persistent molecular objects have attracted a lot of attention lately. Examples include dendrimers,[1,2] hyperbranched structures,[3,4] and comb copolymer(like) molecules.[5,6] In recent years new synthetic routes have been introduced to prepare well-defined comb copolymers. An important breakthrough was achieved by Tsukahara *et al.*,[7,8] who succeeded in polymerizing macromonomers of anionically prepared oligostyrenes. Subsequently, a number of different comb copolymers have been synthesized along this route and their conformations in dilute solutions as well as in thin films were characterized by scattering techniques and atomic force microscopy.[7–11] In a most recent publication a new methodology was introduced and the synthesis, dimensions and solution properties of linear and macro*cyclic* poly(chloroethyl vinyl ether)-*g*-polystyrene comblike copolymers (PCEVE-*g*-PS) were reported.[12]

Experimentally, linear comb copolymers consisting of a flexible backbone densely grafted with flexible side chains have been investigated thoroughly by Schmidt and co-workers.[5,7–11] Another variant uses so-called dendrons as side groups.[6,13] In general, the presence of a large number of side chains results in severe stiffening of the structure leading to cylindrical comb copolymer brushes (or molecular bottle-brushes). These molecules have also been investigated theoretically[14–18] and with computer simulations[19–30] in some detail. Our studies focused mainly on the persistence length as a measure of the stiffness. Important parameters are the grafting density, the flexibility (completely flexible vs rigid rod) of the side chains, the length of the side chains, the size of the side chain ''monomers'' compared to the size of the backbone ''monomers,'' etc. For a fixed grafting density, the persistence length λ is predicted to increase much faster with the length of the side chains (rigid or flexible) than the diameter D of the brush. Consequently, λ/D is predicted to increase strongly with the length of the side chains, thus leading to cylindrically shaped objects with potentially interesting properties (e.g., liquid crystalline solutions).

Computer simulations have been used extensively by Saariaho *et al.*[22,24–27] to address the behavior of λ/D as a function of side chain length for various cases. The influence of the stiffness of the side chains on this ratio was considered in some detail and interesting differences were found between the two cases of completely flexible and rigid rod side chains. Locally, the presence of rigid side chains had no influence at all on the structure of the backbone, whereas flexible side chains lead to severe local stretching. On a larger length scale, characterized by persistence behavior, the persistence length was shown to increase strongly as a function of the side chain length. However, in the regime studied, λ/D was found to be essentially independent of the side chain length for flexible side chains and to increase approximately linearly with side chain length L for rigid side chains. Since theoretically λ/D should ultimately increase linearly in both cases, this scaling regime is apparently obtained much easier with rigid than with flexible side chains. Theoretical arguments supporting this assertion have been put forward.[17,18]

In this paper we will address ring comb copolymers and focus on the influence of the side chain length on the conformational characteristics for a given high grafting density, for flexible and rigid side chains. We will use the elements of the radius of gyration tensor of the backbone to characterize its shape. It is much more difficult to quantify the stiffness of the structure in terms of a persistence length. In case of a linear backbone the persistence length λ is easily identifiable

via the relation $\langle \mathbf{n}(0)\mathbf{n}(s)\rangle = \langle \cos\theta(s)\rangle = \exp(-s/\lambda)$, where $\mathbf{n}(s)$ is the tangential vector to the backbone at position s along the backbone and $\theta(s)$ is the angle between $\mathbf{n}(s=0))$ and $\mathbf{n}(s)$. In the case of a persistence chain forming a ring, such a relation is obviously no longer valid. Still, the behavior of $\langle \mathbf{n}(0)\mathbf{n}(s)\rangle$ as a function of s carries information about the stiffening of the backbone and we will briefly consider this in the limit of stiff rings.

II. MODEL

Off-lattice Monte Carlo (MC) simulations were used to study equilibrium conformations of comb copolymer ring molecules consisting of a flexible closed backbone with either completely flexible or rigid side chains. The ring backbone was modeled as a fully flexible freely jointed chain of 128 or 32 beads, every other of which was grafted with a side chain consisting of beads of the same size as the backbone. The side chain beads are either freely jointed together (flexible side chains) or jointed under a fixed valence angle of 180° (rigid side chains). The length of the side chains was varied systematically from 2 to 32 beads. We will focus on the behavior of a single isolated molecule in an athermal solvent and, therefore, only intramolecular excluded volume interactions between the beads are taken into account. No attempts have been made to conserve the topology (knot structure) of the ring backbone. However, all snapshots observed always corresponded to the unknotted conformation, which comes as no surprise since the probability for the presence of a knot in a ring polymer of this size (i.e., 128 or 32 beads) in an athermal solvent (even without the presence of side chains) is known to be essentially zero.[31,32] The diameter of the beads is taken as the unit of length. The length of the bonds is also one unit, corresponding to tangent spheres.

Configuration space is sampled according to the Metropolis importance-sampling scheme.[33] The initial conformations were formed as unknotted closed 2D backbone structures (x,y-plane) to which side chains are attached alternatingly pointing in the positive and negative z-direction. Several trial moves were used. We distinguish between side chain moves (moves which only involve beads in a single randomly chosen side chain) and backbone moves which move a portion of the backbone plus all the connected side chains. Only one kind of backbone move is used. Two backbone beads are chosen randomly and subsequently, the part of the backbone between these beads is rotated around the axis through the beads chosen. All side chains attached to this part of the backbone move in a concerted fashion. The angle of rotation is chosen randomly from an interval $[-\delta_{\max},\delta_{\max}]$. For the flexible side chains four different types of moves are employed. The ''end move'' consists of moving the free end of a side chain subject to the constraint of fixed bond length. The ''bead rotation'' consists of rotating a single bead around the axis through its neighbors. The ''chain shift'' consists of translating the end part of the side chains. Finally, the ''pivot move'' consists of rotating a set of connected beads. These motions have been described in detail in our previous publications.[22,24–26] For the rigid side chains only one type of side chain move was used. A randomly chosen side chain is given a new orientation, which is chosen isotropically. The relative probability of the different moves has been chosen so as to optimize the sampling procedure.

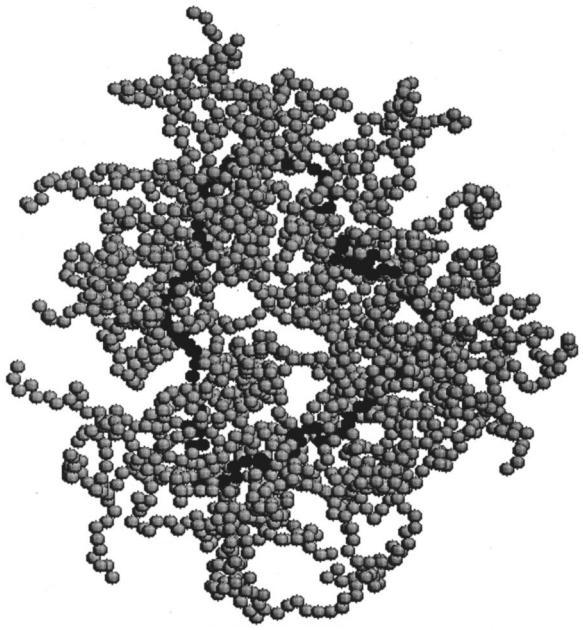

FIG. 1. Snapshot of a ring comb copolymer with a backbone consisting of 128 beads and 64 flexible side chains of length 32. The backbone atoms are colored black.

III. RESULTS AND DISCUSSION

Recently, the dimensions and solution properties of macrocyclic poly(chloroethyl vinyl ether)-*g*- polystyrene comblike copolymers (PCEVE-*g*-PS) were reported.[12] Typically, the cyclic comblike molecules consisted of a PCEVE backbone with a number averaged degree of polymerization $DP_n = 26$ or 56 and approximately 1 polystyrene side chain per backbone monomer. The number averaged molar mass of the polystyrene side chains varied between 2600 and 15200. Consequently, for the cyclic structures considered the size of the side chains (i.e., its end-to-end point distance) can be assumed to be larger than the average diameter of the backbone ring. This feature has important consequences for the stiffening of the ring backbone, a phenomenon that is due to the steric interactions between the side chains and which has been discussed in detail for linear comb copolymers. In what follows, we will discuss comb copolymer ring molecules with flexible and rigid side chains and distinguish between the case where the end-to-end point distance of the side chains is smaller and larger than the ''diameter'' of the ring backbone. In all cases the backbone itself is taken to be flexible.

A. ''Short'' flexible side chains

We start by considering the effect of flexible side chains on the conformational properties. The backbone consists of 128 freely jointed beads. Every other bead contains a side chain of length $N_{sc} = 0$, 8, 16 or 32. Hence, there are 64 side chains. A typical snapshot of the largest structure ($N_{sc} = 32$) is presented in Fig. 1. It demonstrates that for this

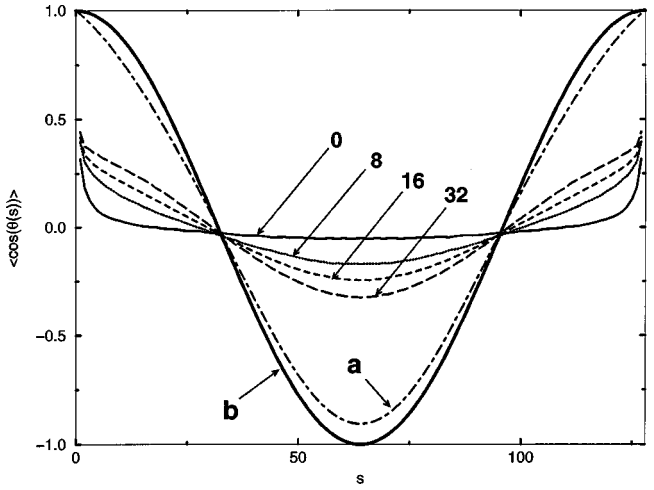

FIG. 2. Directional correlation function $\langle \cos \theta(s) \rangle$ vs s for a backbone of size 128 and 64 side chains of length $N_{sc}=0,8,16,32$. Curve (a) is the analytical result [Eq. (A10)] for a persistent ring of stiffness $\lambda=64$. Curve (b) corresponds to a stiff ring ($\lambda=\infty$).

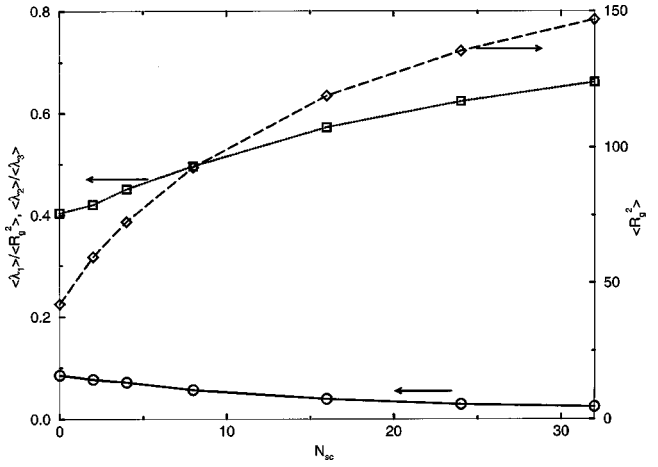

FIG. 3. Backbone dimensions for a ring comb copolymer with a backbone consisting of 128 beads and 64 flexible side chains. The curves show the backbone dimensions vs side chain length. ◇ corresponds to the radius of gyration squared $\langle R_g^2 \rangle$ of the backbone. ○ corresponds to the smallest eigenvalue $\langle \lambda_1 \rangle$ divided by the radius of gyration squared $\langle R_g^2 \rangle$ of the backbone. □ corresponds to the ratio of the middle eigenvalue $\langle \lambda_2 \rangle$ and the largest eigenvalue $\langle \lambda_3 \rangle$.

length of the side chain we are still just within the regime where the end-to-end point distance of the side chains is smaller than the ''diameter'' of the cyclic backbone. The effect of the side chains on the stiffness of the backbone is illustrated in Fig. 2 showing $\langle \mathbf{n}(0)\mathbf{n}(s) \rangle = \langle \cos \theta(s) \rangle$, where $\mathbf{n}(s)$ is the bond vector at position s of the backbone, vs s for the different side chain lengths. Additionally, the result for an ideal ring (circle) is indicated as well as the theoretical result [Eq. (A10)] for a ring with a stiffness corresponding to $L_c=2\lambda$. Although it is impossible to derive a value for the persistence length λ of the backbone from these plots, the increasing stiffness as a function of the side chain length is obvious. Of course, reasonable values for λ are available from the corresponding simulations of linear comb copolymer structures. From these we know that $\lambda \cong 52$, implying that the contour length $L_c \cong 2.5\lambda$. The large difference with the theoretical result is due to two reasons. First, Eq. (A10) cannot really be applied anymore in this regime, since its derivation assumes $\lambda \gg L_c$. But, more importantly, the theoretical model assumes a persistence chain at all length scales, whereas the persistence of the freely jointed bead model simulated only applies at a large length scale, i.e., large values of s. At a short length scale the chain behaves much more flexible, which is clearly demonstrated by the strong drop in $\langle \cos \theta(s) \rangle$ for small values of s and which will be discussed in some detail further on.

The change in conformation of the backbone as a function of the length of the side chains is further illustrated in Fig. 3, showing the square radius of gyration R_g^2 as a function of the side chain length N_{sc}, the ratio λ_1/R_g^2 between the smallest eigenvalue of the radius of gyration tensor of the backbone and the square radius of gyration and the ratio λ_2/λ_3 between the middle and largest eigenvalue. The decrease of λ_1/R_g^2 as a function of N_{sc} indicates an increasing planarity of the structure, whereas the increase of λ_2/λ_3 implies a more circular shape (a perfect ring would correspond to $\lambda_2/\lambda_3=1$). In principle the approach towards a perfectly ring-shaped object should continue taking ever longer side chains, however, for a given backbone length the side chains from one side will start interfering with the side chains from the other side. Hence, longer backbones are required to further follow this process.

B. ''Long'' flexible side chains

Once the end-to-end point distance of the side chains is much longer than the ''diameter'' of the ring backbone we are entering a different regime, which actually corresponds to the situation studied experimentally by Deffieux and co-workers.[12] To investigate this regime we took a backbone of 32 beads with 16 side chains of length 8, 16, 32, and 64, respectively, the latter two clearly being in the ''long'' side chains regime as is illustrated clearly by Fig. 4 presenting a typical snapshot of the largest structure. This situation can be analyzed theoretically at least semiquantitatively. To do this we assume for the sake of the argument that as a zeroth approximation the backbone conformation can be considered as some kind of spherical object to which the side chains are attached, i.e., the many-haired ball picture considered by Witten and Pincus.[34] According to their analysis the free energy of the stretched side chains is given by

$$F \approx \nu T f^{3/2} \ln[M(d/R)(a/d)^{1/\nu}]. \tag{1}$$

Here, $\nu=3/5$ is the Flory exponent, M is the length of the side chains expressed in number of beads of size a, R is the radius of the ball (in our case of the order of the radius of gyration of the backbone), f denotes the number of side chains, and d is the average distance between nearest neighbor side chains (approximately $Rf^{-1/2}$). In our case we should add the free energy of the backbone, which is a function of the size R, and minimize the thus obtained expression with respect to R. It is easily verified that whatever expression is taken for the free energy of the backbone, R will turn out to be independent of M. Hence if the side chains are long enough, the conformational characteristics of the ring back-

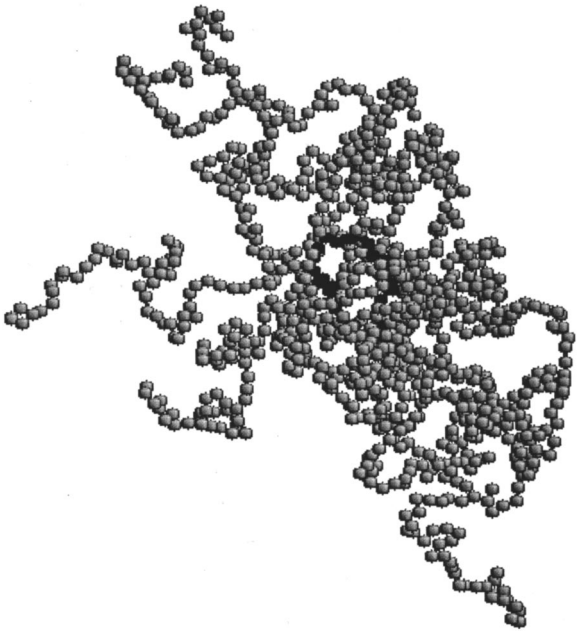

FIG. 4. Snapshot of a ring comb copolymer with a backbone consisting of 32 beads and 16 flexible side chains of length 64. The backbone atoms are colored black.

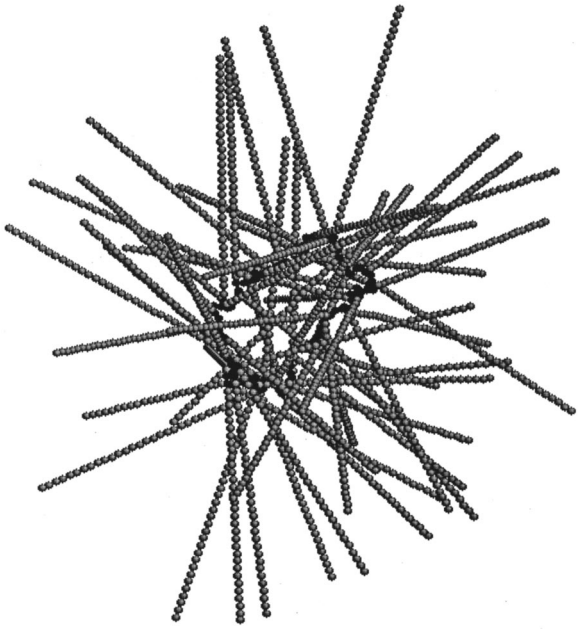

FIG. 6. Snapshot of a ring comb copolymer with a backbone consisting of 128 beads and 64 rigid side chains of length 32. The backbone atoms are colored black.

bone should become independent of the length of the side chains. That this is really the case is demonstrated by the results presented in the following figure (Fig. 5).

C. Rigid rod side chains

In our publications devoted to linear comb copolymer cylindrical brushes it was demonstrated that the flexibility of the side chains plays an important role regarding the side chain induced stiffness of the structure. The stiffer the side chains, the larger the persistence length of the comb copolymer molecule.[26] Hence, rigid rod side chains turn out to be most effective in this respect. However, in the case of ring comb copolymers with rigid rod side chains, overlap between side chains from opposite sides of the ring backbone is almost inevitable unless extremely long backbones are used. In our simulations we used again a backbone of 128 beads and rigid rod side chains of lengths 2, 4, 8, 16, 24, and 32. From these only the first three correspond to a situation where side chains from opposite side do not severely interfere. The last two correspond to the opposite situation. This is clearly illustrated in the next figure showing a typical snapshot for rigid rod side chains of length 32 (Fig. 6). Figure 7 shows the square radius of gyration of the backbone as

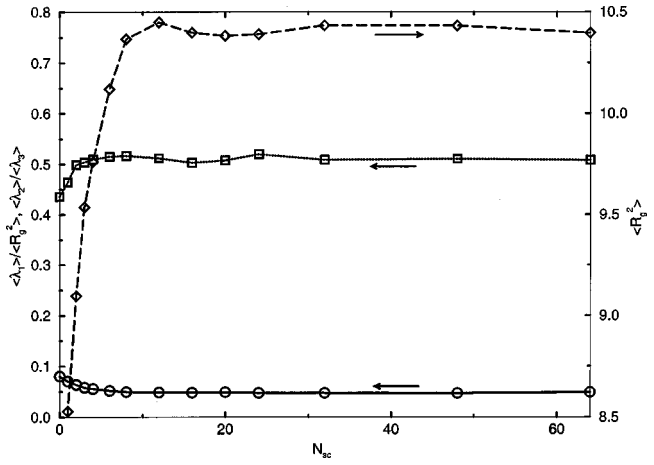

FIG. 5. Backbone dimensions for a ring comb copolymer with a backbone consisting of 32 beads and 16 flexible side chains. The curves show the backbone dimensions vs side chain length. ◇ corresponds to the radius of gyration squared $\langle R_g^2 \rangle$ of the backbone. ○ corresponds to the smallest eigenvalue $\langle \lambda_1 \rangle$ divided by the radius of gyration squared $\langle R_g^2 \rangle$ of the backbone. □ corresponds to the ratio of the middle eigenvalue $\langle \lambda_2 \rangle$ and the largest eigenvalue $\langle \lambda_3 \rangle$.

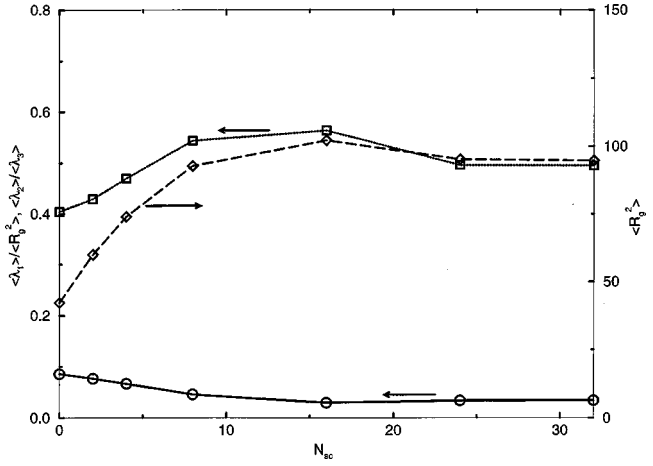

FIG. 7. Backbone dimensions for a ring comb copolymer with a backbone consisting of 128 beads and 64 rigid side chains. The curves show the backbone dimensions vs side chain length. ◇ corresponds to the radius of gyration squared $\langle R_g^2 \rangle$ of the backbone. ○ corresponds to the smallest eigenvalue $\langle \lambda_1 \rangle$ divided by the radius of gyration squared $\langle R_g^2 \rangle$ of the backbone. □ corresponds to the ratio of the middle eigenvalue $\langle \lambda_2 \rangle$ and the largest eigenvalue $\langle \lambda_3 \rangle$.

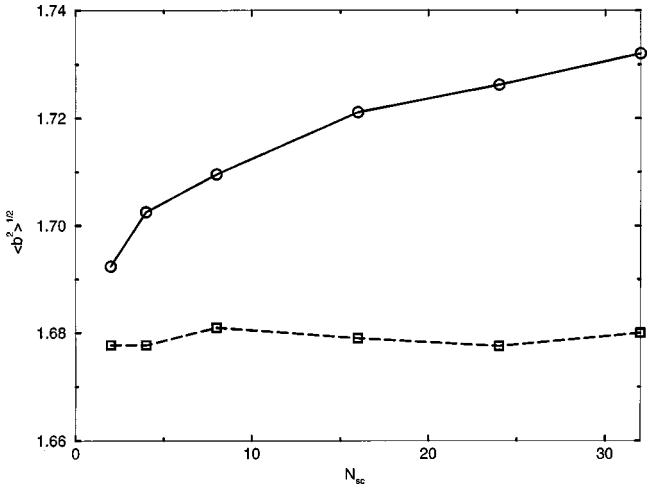

FIG. 8. Distance between neighboring grafted backbone atoms for a ring comb copolymer with a backbone consisting of 128 beads and 64 side chains. ○ corresponds to flexible sidechains. □ corresponds to rigid sidechains.

a function of the side chain length. Clearly, as in the case of flexible side chains, the backbone conformation attains a limiting character once the side chains are sufficiently long. This is also confirmed by the behavior of the eigenvalues of the radius of gyration tensor of the backbone as function of the length of the side chains presented in the same figure. In the case of rigid rod side chains, it is rather straightforward to demonstrate that the excluded volume between two rods approaches a limiting value for side chains that are much longer than the ''diameter'' of the ring backbone.

The most striking observation in the case of linear comb copolymers was that although rigid rod side chains gave rise to a much larger persistence length than flexible side chains, on a small length scale the opposite happened. Rigid rod side chains have no influence at all on the very local backbone fluctuations, whereas flexible side chains lead to local chain stretching which increases with increasing side chain length. Of course the same effect should be expected for ring comb copolymers. The next figure (Fig. 8) shows the average distance b between two consecutive main chain grafting points of the ring comb copolymer brush in the case of flexible and rigid rod side chains as a function of the side chain length. As expected, the behavior is identical as in the case of linear comb copolymers; for rigid side chains b remains constant, whereas for flexible side chains b increases continuously.

In summary, we conclude that although it is in principle possible to create shape persistent donutlike objects using ring comb copolymers, in practice this will be very hard to realize due to the interference between side chains of ''opposite'' sides. This is particularly true because the most effective stiffness inducing side chains are rigid side chains.

APPENDIX

In this appendix we consider the correlation between the tangential vectors $\mathbf{n}(0)$ and $\mathbf{n}(s)$ of a persistence ring polymer characterized by a persistence length λ. It is well known that for a linear persistence chain

$$\langle \mathbf{n}(0)\mathbf{n}(s)\rangle = \langle \cos\theta(s)\rangle = \exp(-s/\lambda), \tag{A1}$$

where $\theta(s)$ is the angle between $\mathbf{n}(s=0)$ and $\mathbf{n}(s)$. Generally, for a ring polymer the problem is very complicated. Therefore, we will restrict the analysis to the case where the persistence length λ is much larger than the contour length L_c, $\lambda \gg L_c$. Obviously, the situation of minimal elastic free energy corresponds to a circular shape of the ring (we ignore complications due to twisting). We will consider the two-dimensional situation where the tangential vector $\mathbf{n}(s) = (\cos\theta(s), \sin\theta(s))$. The circular shape implies that in the 0th approximation $\theta_0(s) = 2\pi s/L_c$ and hence that for the ideal ring

$$\langle \cos\theta(s)\rangle = \cos\theta_0(s) = \cos\frac{2\pi s}{L_c}. \tag{A2}$$

In order to calculate corrections to Eq. (A2), we have to take fluctuations into account based on the increase in elastic energy U_{el} of the deformed circle,

$$U_{\mathrm{el}} = k_B T \frac{\lambda}{4} \int_0^{L_c} \left(\frac{d\mathbf{n}(s)}{ds} \right)^2 ds. \tag{A3}$$

We will fix two angles $\theta(0)=0$ and $\theta(s=s^*)=\theta^*$ and calculate the probability that the chain trajectory actually passes through these points. To this end we will determine the chain trajectory passing through these points and having the minimal elastic energy. Hence, this elastic energy will be a function of s^* and θ^*, $U_{\mathrm{el}} = U_{\mathrm{el}}(s^*, \theta^*)$. In the zeroth approximation,

$$U_{\mathrm{el}}^0 = k_B T \frac{\pi^2 \lambda}{L_c}, \tag{A4}$$

and the distribution function $p(s^*, \theta^*)$ of the deformed circle with fixed angles $\theta(s=0)=0$ and $\theta(s=s^*)=\theta^*$ can be written in the Boltzmann form,

$$p(s^*, \theta^*) = C \exp[-(U_{\mathrm{el}}(s^*, \theta^*) - U_{\mathrm{el}}^0)/k_B T], \tag{A5}$$

where C is the normalization constant.

To find the trajectory with the minimal elastic energy passing through these points the following constraints have to be satisfied:

$$\theta(s=L_c) = 2\pi; \quad \int_0^{L_c} \sin\theta(s)\, ds = 0;$$

$$\int_0^{L_c} \cos\theta(s)\, ds = 0. \tag{A6}$$

Minimization of Eq. (A3) under these constraints results in

$$\frac{\lambda}{2} \frac{d^2\theta(s)}{ds^2} = \mu_2 \cos\theta(s) - \mu_1 \sin\theta(s), \tag{A7}$$

where μ_1 and μ_2 are Lagrange multipliers. To solve our problem Eq. (A7) has to be considered for two different parts, $0 \leqslant s \leqslant s^*$ and $s^* \leqslant s \leqslant L_c$, which results in the following integral equations for $\theta = \theta(s)$:

$$\frac{2s}{\sqrt{\lambda}} = \int_0^{\theta} \frac{d\theta'}{\sqrt{C_1 + \mu_1 \cos\theta' + \mu_2 \sin\theta'}}; \quad 0 \leqslant s \leqslant s^*, \tag{A8a}$$

$$\frac{2(s-s^*)}{\sqrt{\lambda}} = \int_{\theta^*}^{\theta} \frac{d\theta'}{\sqrt{C_2+\mu_1\cos\theta'+\mu_2\sin\theta'}}; \quad s^* \leqslant s \leqslant L_c, \tag{A8b}$$

where the parameters C_1, C_2, μ_1, μ_2 can be found from Eq. (A6) and the condition $\theta(s=s^*)=\theta^*$.

We will now use a perturbation scheme to calculate these parameters assuming that $|\theta_1^*| \equiv |\theta^* - 2\pi s^*/L_c| \ll 1$, i.e., θ^* is close to $2\pi s^*/L_c$ and the fluctuations are small. The zeroth approximation implies that $C_1=C_2=C_0=\pi^2\lambda/L_c$ and $\mu_1=\mu_2=0$. Assuming therefore that $C_1=C_0+C_1'$, $|C_1'| \ll 1$; $C_2=C_0+C_2'$, $|C_2'| \ll 1$, and $|\mu_1| \ll 1$, $|\mu_2| \ll 1$, we can find the chain trajectory as well as the elastic energy using a simple perturbation scheme. Without presenting the details, this leads to an elastic energy given by

$$U_{\mathrm{el}}(s^*,\theta^*) = U_{\mathrm{el}}^0 + \frac{\lambda}{4}\frac{L_c}{s^*(L_c-s^*)}\frac{\theta^{*2}}{1-\dfrac{2L_c^2\sin^2(\pi s^*/L_c)}{\pi^2 s^*(L_c-s^*)}}. \tag{A9}$$

After substitution of this energy in Eq. (A5) for the distribution function we obtain a Gaussian function for which the average $\langle\cos\theta(s^*)\rangle = \langle\cos\theta^*\rangle$ can be easily calculated,

$$\langle\cos\theta(s^*)\rangle = \cos\frac{2\pi s^*}{L_c}\left(1-\frac{L_c}{\lambda}\left(\frac{s^*(L_c-s^*)}{L_c^2} - \frac{2}{\pi^2}\sin^2\left(\frac{\pi s^*}{L_c}\right)\right)\right) \tag{A10}$$

which is the functional form used in the text to compare with the numerical results.

[1] D. A. Thomalia, Adv. Mater. **6**, 529 (1994).
[2] J. M. J. Fréchet, Science **263**, 1710 (1994).
[3] E. Malmström and A. Hult, J. M. S.-Rev. Macromol. Chem. Phys. **C37**, 555 (1997).
[4] Y. H. Kim, J. Polym. Sci., Part A: Polym. Chem. **36**, 1685 (1998).
[5] S. S. Sheiko, M. Gerle, K. Fischer, M. Schmidt, and M. Möller, Langmuir **13**, 5368 (1997).
[6] V. Percec, C.-H. Ahn, G. Ungar, D. S. P. Yeardley, M. Möller, and S. S. Sheiko, Nature (London) **391**, 161 (1998).
[7] M. Wintermantel, M. Schmidt, Y. Tsukahara, K. Kajiwara, and S. Kohjiya, Macromol. Rapid Commun. **15**, 279 (1994).
[8] M. Wintermantel, M. Gerle, K. Fischer, M. Schmidt, I. Wataoka, H. Urakawa, K. Kajiwara, and Y. Tsukahara, Macromolecules **29**, 978 (1996).
[9] P. Dziezok, S. S. Sheiko, K. Fischer, M. Schmidt, and M. Möller, Angew. Chem. **109**, 2894 (1997).
[10] S. A. Prokhorova, S. S. Sheiko, M. Möller, C.-H. Ahn, and V. Percec, Macromol. Rapid Commun. **19**, 359 (1998).
[11] M. Gerle, K. Fischer, S. Roos, A. H. E. Müller, M. Schmidt, S. S. Sheiko, S. Prokhorova, and M. Möller, Macromolecules **32**, 2629 (1999).
[12] M. Schappacher, C. Billaud, C. Paulo, and A. Deffieux, Macromol. Chem. Phys. **200**, 2377 (1999).
[13] A. D. Schlüter and J. P. Rabe, Angew. Chem. Int. Ed. Engl. **39**, 864 (2000).
[14] T. M. Birshtein, O. V. Borisov, E. B. Zhulina, A. R. Khokhlov, and T. A. Yurasova, Polym. Sci. U.S.S.R. **29**, 1293 (1987).
[15] G. H. Fredrickson, Macromolecules **26**, 2825 (1993).
[16] Y. Rouault and O. V. Borisov, Macromolecules **29**, 2605 (1996).
[17] A. Subbotin, M. Saariaho, O. Ikkala, and G. ten Brinke, Macromolecules **33**, 3447 (2000).
[18] A. Subbotin, M. Saariaho, R. Stepanyan, O. Ikkala, and G. ten Brinke, Macromolecules **33**, 6168 (2000).
[19] L. V. Gallacher and S. Windwer, J. Chem. Phys. **44**, 1139 (1966).
[20] J. E. G. Lipson, Macromolecules **24**, 1327 (1991).
[21] A. Gauger and T. Pakula, Macromolecules **28**, 190 (1995).
[22] M. Saariaho, O. Ikkala, I. Szleifer, I. Erukhimovich, and G. ten Brinke, J. Chem. Phys. **107**, 3267 (1997).
[23] Y. Rouault, Macromol. Theory Simul. **7**, 395 (1998).
[24] M. Saariaho, I. Szleifer, O. Ikkala, and G. ten Brinke, Macromol. Theory Simul. **7**, 211 (1998).
[25] M. Saariaho, O. Ikkala, and G. ten Brinke, J. Chem. Phys. **110**, 1180 (1999).
[26] M. Saariaho, A. Subbotin, I. Szleifer, O. Ikkala, and G. ten Brinke, Macromolecules **32**, 4439 (1999).
[27] M. Saariaho, A. Subbotin, O. Ikkala, and G. ten Brinke, Macromol. Rapid Commun. **21**, 110 (2000).
[28] P. G. Khalatur and A. R. Khokhlov, J. Chem. Phys. **112**, 4849 (2000).
[29] P. G. Khalatur, D. G. Shirvanyanz, N. Yu. Starovoitova, and A. R. Khokhlov, Macromol. Theory Simul. **9**, 141 (2000).
[30] K. Shiokawa, K. Itoh, and N. Nemoto, J. Chem. Phys. **111**, 8165 (1999).
[31] M. D. Frank-Kamenetskii, A. V. Lukashin, and A. V. Vologodskii, Nature (London) **258**, 398 (1975).
[32] K. Koniaris and M. Muthukumar, J. Chem. Phys. **95**, 2873 (1991).
[33] N. Metropolis, A. W. Rosenbluth, M. N. Rosenbluth, A. H. Teller, and E. Teller, J. Chem. Phys. **21**, 1087 (1953).
[34] T. A. Witten and P. A. Pincus, Macromolecules **19**, 2509 (1986).